ORGANIC LETTERS

2013
Vol. 15, No. 6
1330–1333

Turn-On, Fluorescent Nuclear Stains with Live Cell Compatibility

Demar R. G. Pitter,[†] Jens Wigenius,[‡] Adrienne S. Brown,[†] James D. Baker,[§] Fredrik Westerlund,*[,‡] and James N. Wilson*[,†]

Departments of Chemistry and Biology, University of Miami, 1301 Memorial Drive, Coral Gables, Florida 33146, United States, and Department of Chemical & Biological Engineering, Chalmers University of Technology, 412 96 Gothenburg, Sweden

fredrik.westerlund@chalmers.se; jnwilson@miami.edu

Received January 29, 2013

ABSTRACT

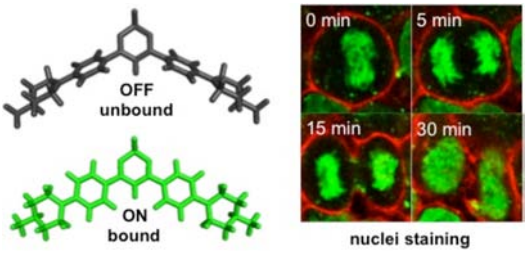

DNA-binding, green and yellow fluorescent probes with excellent brightness and high on/off ratios are reported. The probes are membrane permeable, live-cell compatible, and optimally matched to 405 nm and 514 nm laser lines, making them attractive alternatives to UV-excited and blue emissive Hoechst 33342 and DAPI nuclear stains. Their electronic structure was investigated by optical spectroscopy supported by TD-DFT calculations. DNA binding is accompanied by 27- to 75-fold emission enhancements, and linear dichroism demonstrates that one dye is a groove binder while the other intercalates into DNA.

Fluorescent nuclear stains are widely employed in cell life cycle analysis and flow cytometry and as counterstains in fluorescence microscopy.[1,2] Probes possessing well-defined binding modes also find applications in quantification of nucleic acids[2,3] as well as investigations into the statistical-mechanical properties,[4] solution orientation, and dynamics of DNA.[5] Despite the availability of several classes of fluorescent nuclear stains, there remain limitations to their universal application due to available excitation wavelengths,[2,6] membrane permeability,[7] and toxicity.[8,9] Indole and benzimide vital dyes, such as DAPI and Hoechst 33342, possess excitation maxima in the UV that are poorly matched to visible laser lines.[2,6] On the other hand, DNA-intercalating carbocyanine dyes,[10] such as TOTO or YOYO,[11] offer long wavelength excitation and emission but require cell fixation and permeabilization.[12]

In this letter, we report two novel fluorescent nuclear stains: 4,6-bis(4-(4-methylpiperazin-1-yl)phenyl) pyrimidin-2-ol, **1**, and [1,3-bis[4-(4-methylpiperazin-1-yl)phenyl]-1,3-propandioato-κO, $\kappa O'$] difluoroboron, **2** (Figure 1). Optical spectroscopy reveals that they are optimally matched to available 405 nm (**1**) and 514 nm (**2**) laser lines and are also compatible with standard filter sets. DNA binding was investigated by fluorescence and flow-aligned linear

[†] University of Miami, Department of Chemistry.
[‡] Chalmers University of Technology.
[§] University of Miami, Department of Biology.

(1) Suzuki, T.; Fujikura, K.; Higashiyama, T.; Takata, K. *J. Histochem. Cytochem.* **1997**, *45*, 49–53.
(2) Ploeger, L. S.; Dullens, H. F.; Huisman, A.; van Diest, P. J. *Biotech. Histochem.* **2008**, *83*, 63–69.
(3) Darzynkiewicz, Z. *Current Protocols in Cytometry*; John Wiley & Sons: 2010; Ch. 7.
(4) Gunther, K.; Mertig, M.; Seidel, R. *Nucleic Acids Res.* **2010**, *38*, 6526–6532.
(5) Persson, F.; Westerlund, F.; Tegenfeldt, J. O.; Kristensen, A. *Small* **2009**, *5*, 190–193.
(6) Glaser, K.; Wilke, K.; Wepf, R.; Biel, S. S. *Skin Res. Technol.* **2008**, *14*, 324–326.
(7) Nocker, A.; Sossa-Fernandez, P.; Burr, M. D.; Camper, A. K. *Appl. Environ. Microbiol.* **2007**, *73*, 5111–5117.
(8) Zhao, H.; Traganos, F.; Dobrucki, J.; Wlodkowic, D.; Darzynkiewicz, Z. *Cytometry A* **2009**, *75*, 510–519.
(9) Huang, X.; King, M. A.; Halicka, H. D.; Traganos, F.; Okafuji, M.; Darzynkiewicz, Z. *Cytometry A* **2004**, *62*, 1–7.
(10) Armitage, B. A. *Top. Curr. Chem.* **2005**, *253*, 55–76.
(11) Hirons, G. T.; Fawcett, J. J.; Crissman, H. A. *Cytometry* **1994**, *15*, 129–140.
(12) Bink, K.; Walch, A.; Feuchtinger, A.; Eisenmann, H.; Hutzler, P.; Hofler, H.; Werner, M. *Histochem. Cell. Biol.* **2001**, *115*, 293–299.

10.1021/ol400268t
Published on Web 03/05/2013

dichroism (flow-LD) spectroscopy. Both dyes exhibit high on/off ratios with improved brightness over DAPI and Hoechst dyes. This enables lower dye loadings and/or illumination intensities, which, coupled to their low cytotoxicity, makes **1** and **2** attractive alternatives to existing nuclear stains.

1 and **2** were designed as DNA-targeting, 'turn-on' fluorescent probes and incorporate three key design elements (Figure 1). First, their optical properties are addressed through the incorporation of a donor−acceptor−donor π-system that enables excitation and emission wavelengths in the visible spectrum as well as high sensitivity toward their microenvironment.[13,14] Second, the pendant aryl arms control optical switching with emission enhancements expected when rotation is limited. Finally, recognition units may be incorporated via 4-amino positions of the arms; for **1** and **2**, *N*-methylpiperazine was chosen, as, at physiological pH, protonation will result in a dicationic species suitable for electrostatic interactions with the phosphate backbone of DNA. With an aromatic core capable of interacting with nucleobases and charge spacing well matched to the interbackbone phosphate distance of 18.3 Å, we anticipated that **1** and **2** were ideally suited as intercalators, though a groove binding mode is possible as well, due to their concave shape (Figure 1C, D).

1 is the product of the Bignelli reaction of 4-(4-methyl-1-piperazinyl) benzaldehyde, 4-(4-methyl-1-piperazinyl) acetophenone, and urea, isolated in 22% yield as a bright yellow solid. Reaction of 1,3-bis(4-fluorophenyl)-1,3-propanedione with boron trifluoride followed by nucleophilic aromatic substitution with *N*-methylpiperazine afforded **2** as a bright orange solid in an overall yield of 11%. **1** And **2** were characterized by ^{1}H NMR, ^{13}C NMR, HRMS, and IR (see Supporting Information).

Absorption and emission spectroscopy demonstrate that **1** and **2** are responsive to their chemical environment (Table 1). Both probes show moderate absorption enhancements in methanol and octanol compared to phosphate buffered saline (PBS). The absorption maximum of **2** is bathochromically shifted by 70 nm relative to **1** in all the solvents examined. As both dyes possess the same electron-donating arms, the red shift observed for **2** is the result of a lower energy LUMO due to the increased electron-withdrawing ability of the propandionato-difluoroboron core.

The emission of **1** is enhanced 80-fold in octanol compared to PBS, while, for **2**, a 30-fold enhancement was observed. The emission maxima of **1** range from 475 nm in octanol to 511 nm in ethylene glycol, and the emission maxima of **2** vary from 523 nm in methanol to 553 nm in ethylene glycol. The solvent-dependent emission enhancement is likely the result of the donor−acceptor π-system that yields an excited state with charge transfer (CT) character, while the rotational freedom of the pendant aryl arms may contribute to a twisted intramolecular CT (TICT) excited state. Φ_{em} appears to correlate with solvent polarity and is higher in less polar solvents (octanol > methanol > ethylene glycol > PBS).

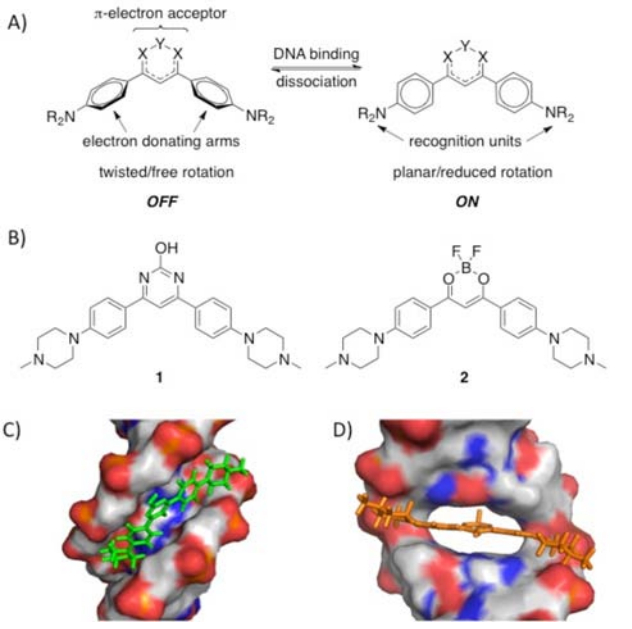

Figure 1. (A) Design strategy for DNA-binding, turn-on probes includes a donor-π-acceptor core, rotatable arms that control emission, and *N*-methylpiperazine recognition units to interact with the phosphate backbone. (B) Chemical structures of **1** and **2**. Possible modes of interaction of the protonated species with DNA include (C) groove binding or (D) intercalation.

Table 1. Optical Data for **1** and **2**

	$\lambda_{max,\ abs}$ nm	ε M^{-1}, cm^{-1}	$\lambda_{max,\ em}$ nm	Δν cm^{-1}	Φ_{em}
PBS					
1	388	35,000	502	5850	0.003
2	469	40,000	535	2600	0.006
ethylene glycol					
1	410	33,000	511	4800	0.03
2	492	44,000	553	2200	0.05
MeOH					
1	392	39,000	493	5230	0.04
2	455	50,000	523	2860	0.07
octanol					
1	399	42,000	475	4010	0.24
2	464	51,000	527	2600	0.18
ctDNA[a]					
1	392	28,000	504	4200	0.11
2	472	38,000	556	3200	0.06
DAPI	350	22,000	451	6400	0.57
Hoechst[b]	350	47,000	452	6400	0.82

[a] [ctDNA] = 50 μM in PBS, [dye] = 1.0 μM in PBS. [b] Hoechst 33342.

TD-DFT calculations (B3LYP 6-31G(d)) provide insights into the electronic structure responsible for the observed optical properties. **1** And **2** are largely isoelectronic with respect to their frontier molecular orbitals and related electronic transitions which is not surprising given their similar architecture (Figure 2). The relevant excited states with significant oscillator strength (f > 0.10) are shown in

(13) Adjaye-Mensah, E.; Gonzalez, W. G.; Bussé, D. R.; Captain, B.; Miksovska, J.; Wilson, J. N. *J. Phys. Chem. A* **2012**, *116*, 8671–8677.
(14) Dhuguru, J.; Gheewala, C.; Kumar, N. S. S.; Wilson, J. N. *Org. Lett.* **2011**, *13*, 4188–4191.

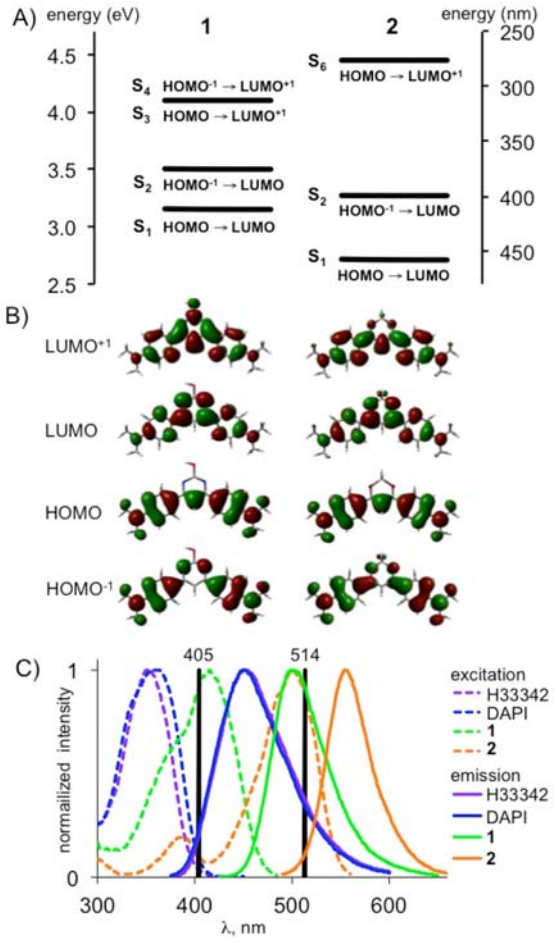

Figure 2. (A) Excited state manifold with relevant contributing molecular orbitals indicated TD-DFT B3LYP/6-31G(d) in MeOH using the SMD solvent model. (B) Frontier (±1) molecular orbitals; 4-methylpiperazine is truncated to dimethyl amino groups. (C) Excitation and emission of **1** and **2** compared to Hoechst 33342 and DAPI bound to ctDNA; the 405 nm and 514 nm laser lines are indicated.

Figure 2A. The calculated transition $S_0 \rightarrow S_1$ energies of 394 nm for **1** and 467 nm for **2** are in very good agreement with the experimentally observed values (Table 1). Both the HOMO and HOMO^{-1} exhibit greater orbital contributions from the pendant aryl arms, while the LUMO shows a greater contribution from the electron-withdrawing core. The polarization of the HOMO and LUMO confirms the notion of an excited state with CT character[15] which has been previously described for structurally related 4,6-diaryl-pyrimidones.[13,14] This CT state should be stabilized in polar solvents leading to the observed fluorescence quenching.

We next examined the optical response of **1** and **2** upon exposure to calf thymus DNA (ctDNA). It was anticipated that probes interacting with DNA, either in a groove-binding mode or as intercalators, would experience a less polar and/or more restrictive environment in which quenching processes would be limited.[10,13,16] In the presence of ctDNA, emission of the probes increases substantially: a 40-fold increase was found for **1** and a 10-fold increase for **2** (Table 1) based on quantum yields. Interestingly, the excitation spectra of the bound probes were bathochromically shifted relative to the absorption maxima; in the case of **1**, $\lambda_{max,\ abs} = 392$ nm and $\lambda_{max,\ ex} = 415$ nm, while, for **2**, $\lambda_{max,\ abs} = 472$ nm and $\lambda_{max,\ ex} = 501$ nm. The bathochromic shift effectively increases the on/off ratios of the probes when exciting at the longer wavelengths; for **1** an on/off ratio of 75 is obtained with 405 nm excitation, and for **2** a ratio of 27 is obtained with 514 nm excitation.

In order to investigate the binding mode of **1** and **2** in more detail, we used flow aligned linear dichroism (flow-LD)[17] in which DNA is aligned in a shear flow and the absorption is measured parallel and perpendicular to the flow direction. The DNA bases will be oriented perpendicular to the flow and thus have a strong negative LD signal centered around 260 nm. Any molecule that is bound to DNA will also be aligned and give rise to an LD signal, and the sign and amplitude of the LD signal is related to the angle between its transition dipole moments and the DNA long-axis. The LD spectra for **1** and **2** are quite different with respect to each other in shape and magnitude (Figure 3A), and they also differ from their correspdonding isotropic absorption spectra (Figure 3B–C). For **2** the magnitude of the peak at 475 nm, corresponding to the $S_0 \rightarrow S_1$ transition, indicates that the transition dipole is aligned roughly parallel with the DNA base pairs, an orientation that is consistent with an intercalated binding, as the $S_0 \rightarrow S_1$ transition dipole of **2** lies within the plane of the molecule. To assign the peak to a binding mode in a quantitative manner, we calculated the reduced linear dichroism (LD^r). The LD^r is directly related to the angle between the transition moment and the orientation axis through the following equation:

$$LD^r = LD/A_{iso} = 3/2*S*(3\cos^2\alpha - 1) \qquad (1)$$

where α is the angle between the orientation axis and the transition dipole moment and S is an orientation factor that is identical for DNA and ligands bound to DNA in the same sample. The LD^r for the 475 nm peak of **2** has a value that is very similar to the DNA band, confirming a binding angle close to 90° (Figure 3A).

The LD spectrum of **1** is most readily explained by a dominant groove-binding mode since the main transition at 410 nm gives rise to a very weak LD signal and an LD^r value close to 0. Interestingly we observe a distinct negative peak at 360 nm that is barely visible in the isotropic absorption and corresponds to the weak $S_0 \rightarrow S_2$ transition ($f = 0.11$). This transition dipole is oriented perpendicular to the $S_0 \rightarrow S_1$ transition dipole (Figure 3D), and its stronger negative LD suggests that it is nearly perpendicular to the DNA helix axis. This is in good agreement with groove

(15) Zucchero, A. J.; McGrier, P. L.; Bunz, U. H. F. *Acc. Chem. Res.* **2010**, *43*, 397–408.

(16) Wilson, J. N.; Brown, A. S.; Babinchak, W. M.; Ridge, C. D.; Walls, J. D. *Org. Biomol. Chem.* **2012**, *10*, 8710–8719.

(17) Norden, B.; Kubista, M.; Kurucsev, T. *Q. Rev. Biophys.* **1992**, *25*, 51–170.

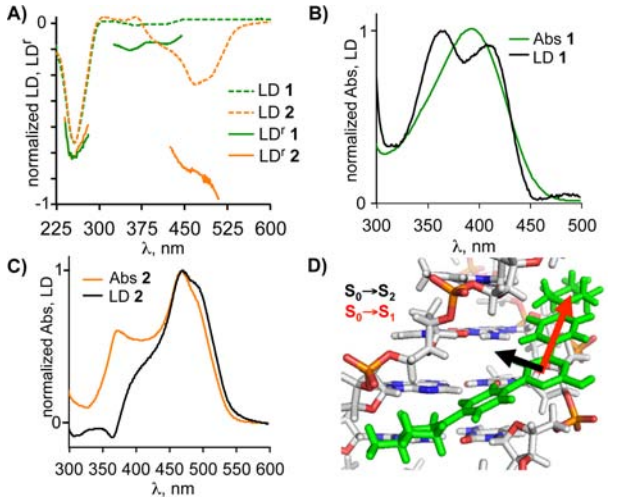

Figure 3. (A) LD and LD^r spectra for **1** and **2** bound to ct-DNA, normalized at 260 nm. Comparison of the normalized LD and isotropic absorption spectra of (B) **1** and (C) **2**. (D) Possible orientation of the $S_0 \rightarrow S_1$ (red) and $S_0 \rightarrow S_2$ (black) transition dipoles of groove-bound **1** based on the LD^r spectra.

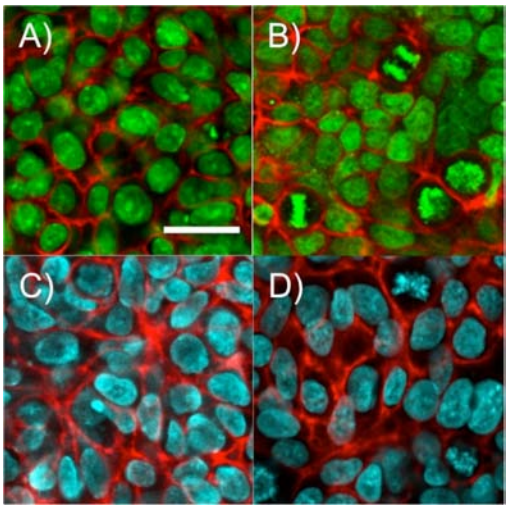

Figure 4. Comparison of nuclei stained with **1** and **2** (top) versus Hoechst 33342 and DAPI (bottom): (A) **1** with HEK293 cells, (B) **2** with MCF7 cells, (C) Hoechst 33342 with HEK293 cells, and (D) DAPI with HEK293 cells; CellMask Deep Red (Life Technologies) is the membrane stain; scale bar = 20 μm.

binding, since such a binding geometry would position the $S_0 \rightarrow S_2$ tranistion parallel to the DNA bases (Figure 3D). The LD^r for the $S_0 \rightarrow S_1$ transition corresponds to an angle of 57°, and while this is slightly larger than that for typical groove binders such as DAPI,[18] it may be the result of major groove binding where a slightly larger binding angle is possible.

The performance of **1** and **2** as nuclear stains was evaluated using two common cell lines, HEK 293 and MCF-7. Representative images of **1** (λ_{ex} = 405 nm) with HEK 293 cells and **2** (λ_{ex} = 514 nm) with MCF-7 cells are shown in Figure 4. Both **1** and **2** were found to illuminate cell nuclei in a manner consistent with DAPI and Hoechst 33342 staining. For all imaging experiments cells were not fixed, no antifade reagent was used, and no rinsing was necessary to remove nonfluorescent unbound probe; optimum probe concentration was found to be in the range of 1 to 10 μM. The higher molar absorptivity of **1** at 405 nm makes it 6 to 10 times brighter than either DAPI or Hoechst 33342 at identical dye loadings and optical settings. The improved brightness of the probes allows for lower illumination intensities and/or dye loading, which is useful for prolonged imaging experiments using live cells or tissue. Both **1** and **2** exhibit low cytotoxicity: cells cultured in media with probe concentrations of 1.0 μM or less do not differ from untreated cells in time to confluence, while higher probe concentrations, between 2.5 and 10 μM, are tolerated for up to 24 h. Longer exposure to **2** does lead to vesicular accumulation in cells that otherwise appear healthy and continue to grow normally; no such accumulation was found for **1**.

In conclusion, we have designed and synthesized two DNA-binding, turn-on fluorescent probes that function as live cell compatible nuclear stains. Optical spectroscopy shows that **1** and **2** exhibit emission enhancements upon exposure to nonpolar solvents and ctDNA. Linear dichroism studies reveal that, despite their isoelectronic structures, **1** is predominantly a groove binder while **2** is an intercalator. We have demonstrated their use in live cells, and both probes were found to be membrane permeable, exhibit low toxicity, and selectively stain cell nuclei. Overall the dyes compare favorably to widely employed vital nuclear stains DAPI and Hoechst 33342 in terms of brightness, photostability, and compatibility with common laser lines.

Acknowledgment. This work was supported by the Bankhead-Coley Biomedical Research Program, 3BN08 (J.N.W.) and by the Chalmers Area of Advance in Nanoscience and Nanotechnology and the Swedish Foundation for Strategic Research (F.W.)

Supporting Information Available. Synthesis and characterization of **1** and **2**; details of optical spectroscopy, TD-DFT calculations, and confocal microscopy. This material is available free of charge via the Internet at http://pubs.acs.org.

(18) Larsson, A.; Åkerman, B.; Jonsson, M. *J. Phys. Chem.* **1996**, *100*, 3252–3263.

The authors declare no competing financial interest.